Proceedings of the ASME 2010 3rd Joint US-European Fluids Engineering Summer Meeting and 8th International Conference on Nanochannels, Microchannels, and Minichannels
FEDSM-ICNMM2010
August 1-5, 2010, Montreal, Canada

FEDSM-ICNMM2010-30944

EFFECT OF DIFFUSER CONTRACTION FOR CENTRIFUGAL COMPRESSOR

Kyung-Jun Kang
Energy mechanics center,
Korea institute of science and technology
, Republic of Korea
Kkj79@kist.re.kr

You-Hwan Shin
Energy mechanics center,
Korea institute of science and technology
, Republic of Korea
yhshin@kist.re.kr

Kwang-Ho Kim
Energy mechanics center,
Korea institute of science and technology
, Republic of Korea
khkim@kist.re.kr

Yoon-Pyo Lee
Energy mechanics center,
Korea institute of science and technology
, Republic of Korea
yplee@kist.re.kr

ABSTRACT

This study will be described details on influence of movable diffuser such as local reverse flow patterns and pressure fluctuation in a vaneless diffuser during unstable operation of a centrifugal compressor. The experimental study is carried out in centrifugal compressor immersed into a water reservoir. Particle Image Velocity (PIV) is used to observe a secondary flow pattern and pressure transducer is used for investigating the onset and development of rotating stall inside vaneless diffuser. The reverse flow zone observes near hub wall of impeller exit at relatively low flow rate. This reverse flow on hub side wall brings about the rotating stall.

This paper be simultaneously discussed on the effects of diffuser contraction to remove local reverse flow zone near hub wall, which are including variation of flow field in a vaneless diffuser and the influence on the pressure fluctuation. A contraction due to movable diffuser three cases (40%, 53% and 86% of diffuser width) was inserted into vaneless diffuser from a shroud wall. According to the results, the rotating stall involving single and two cells is enveloped by the outer lobe of the Rossby wave. Under the rotating stall onset, the stall propagation rate is 1.25Hz, 25% of the impeller speed in the same direction as the impeller in case of no contraction. In case of 40% contraction, onset of rotating stall is not delayed. In contrast of that, onset of rotating stall is delayed in case of 53%, 87% contraction.

There exist several secondary vortices inside vaneless diffuser under onset of rotating stall. The size and location of them vary as flow rate decreases.

Keywords: Movable diffuser, PIV, Centrifugal compressor, Rotating stall, Secondary flow, Vaneless diffuser.

INTRODUCTION

Some phenomena such as rotating stall and surge makes a performance of turbomachinery reduce. A rotating stall may occur in the parallel wall vaneless diffuser of a centrifugal compressor at low flow rate region and become unstable. The phenomenon of rotating stall can occur in any component or a combination of components (such as impeller, vane and vaneless diffuser) of the radial compression system. Rotating stall is widely recognized by self-induced circumferential flow distortions which may rotate around the periphery of the component in which it takes place. The rotating stall in comparatively low flow rate may be induced by reverse flow under strongly adverse pressure gradient. The secondary vortices due to reverse flow bring about a local loss and blocking of through flow in vaneless diffuser.

Many studies have been done in order to understand the nature of rotating stall. Jasen (1964) has developed a theory and has pointed out the instability of the reverse flow layer on the diffuser wall. Nagashima et al.(1989) proposed that rotating stall is caused by the disturbance that develops in the reversed flow regions on the shroud and hub wall near the diffuser inlet as the flow rate approaches the critical value for occurrence of rotating stall. Tsurusaki et al. (1999) have examined the reverse flow and the rotating stall and have made clear the flow condition of a fully developed rotating stall.

Investigation of the unsteady characteristics of diffuser flows were reported by Abdelhamid at al.(1982), Senoo and Kinoshita(1983). Detailed flow behavior near or at stall conditions could not be deduced from pressure measurements

alone. It is not known whether these separated zones originate from the hub or from the shroud and how many separated zones are present for a given diffuser and flow condition.

A methods for suppressing the occurrence of rotating stall to expand the stable operation region is an important engineering issue. Suppression of this unstable flow is important key factor for stability of operation and increasing of efficiency on a compressor. In order to delay the rotating stall, various methods have been investigated; throttling at the diffuser exit(1982), recircular cascade diffuser with a low solidity(1983), a combination of the low solidity and IGV(Inlet Guide Vane)(1996), a shallow radial grooves on the diffuser walls(1997), jet injected in the counter-direction of impeller rotation(1999) and wall roughness control vaneless diffuser(2001). Figure 1 shows example of the movable diffuser used in a compressor of chillers. This device is to delay the unstable region and increase in surge margin of compressor. In the case of full load, wake flow appears on shroud wall of impeller suction side. This wake region brings about separation ring on the shroud casing wall. The reverse flow on the shroud side wall enters into the tip clearance and moves upstream along the shroud casing wall toward the separation ring position, then flows into the blade passage again. The stable recirculation flow resulting from three-dimensional separation on the shroud wall does not lead to the rotating stall. As decreases in flow rate, the unstable flow causes that momentum of a radial direction is not large enough to overcome an adverse pressure gradient.

PIV was chosen to analyze and further improve the understanding of the complex flow phenomena inside the vaneless diffuser. PIV (Particle Image Velocimetry) and pressure fluctuation measurements are used for investigation the onset and development of rotating stall within a centrifugal compressor having a vaneless diffuser. In this paper we present results from the simultaneous capture flow field along with dynamic pressure measurements at flow conditions experienced during rotating stall. Objective of this study is to prevent rotating stall using by movable diffuser and clearly identify the processing of it.

EXPERIMENTAL FACILITY

A direct current (DC) low speed geared motor was used. There are 18 backward blades. The diameter of the diffuser is 2.24 times that of the impeller and the distance between the two side walls of the diffuser is 16 mm. The specifications are given in Table 1. The time-averaged flow fields of the *r-z* plane at different heights were measured using PIV (Particle image velocimetry). Flow fields were analyzed with Dantec dynamics autocorrelation software and averaged by 300 image pairs acquired during a period of 60 s. The window size was 64×64 pixels and the vectors were calculated every 32 pixels with 50 percent overlap between neighboring windows.

An argon laser with a maximum power of 5 W was used as the light source. A two-dimensional (2-D) light sheet with a thickness of 1 mm was generated. As shown in Fig. 1(a), the observation region lighted by the laser sheet covered the impeller exit, vaneless diffuser, and collecting chamber. A high speed charge-coupled device (CCD) camera (1280×1024 pixels) was placed over the observation region as shown in Fig. 1(b). The *r-z* plane in the vaneless diffuser was located at circumferential angles of θ = 0°. Circular-shaped polyvinyl chloride (PVC) with a diameter of 40 ㎛ was used for particle for flow tracking. Pressure transducer is used to measure the shroud wall static pressure fluctuations during rotating stall and are arranged in r_o= 0.2 along the circumference of impeller as shown in figure 2(a).

The PIV measurement velocity $V = S\Delta p/\Delta t$, where S, Δp and Δt are particle pixel displacement, optical magnification, and the time delay between the two consecutive images, respectively. Westerweel et al. reported that the average measurement error for an interrogation analysis through cross correlation with window offset was approximately 0.04 pixel. The maximum particle displacement of 6 pixels (one-fourth of the diameter of a 16×16 pixel interrogation window), this would imply a relative measurement error of $\delta(\Delta p)/\Delta p$=1%.

Figure 3 shows the schematic of the movable diffuser inserted into the vaneless diffuser. Parameters of the movable diffuser are depth(=b′/b) of contraction, width and distance between impeller exit and the movable diffuser. In this study, depth of the movable diffuser is considered as most important factor in order to delay the rotating stall. The width of movable diffuser range from r_o=0.12 to 0.18 on shroud wall. The movable diffuser in order to investigate an effect of depth is inserted to 40%, 53% and 87%.

RESULT AND DISCUSSIOIN

Figure 4 shows the comparison of performance characteristics on the flow rate of test compressor. In this performance curve, circle denotes operating line of compressor in case without contraction at rotational speed 300 RPM. Triangle, square and downside up triangle indicate the case of 40%, 53% and 87%, respectively. The four operating points on each line were selected for understanding of development processing of rotating stall in vaneless diffuser. Compressor exit blockage is set using dampering at the exit of compressor. Operating points a, e, i and m are correspond with exit blockage 85%. The exit blockage is slightly decreased to 97% which correspond with operating points d, h, l and p. In the performance characteristics, operating line moves toward low flow rate region and total pressure at the exit of compressor is decreased as the contraction increases. In different operating point, pressure fluctuation and secondary flow pattern will be discussed in later.

Figure. 5 shows the frequency spectra of the pressure fluctuations at different operating point. The pressure signal is obtained from pressure transducer located in #1. In the case without contraction, rotating stall signal appears in operating point a as shown in Fig.5(a). The dominant frequency in rotating stall onset is 1.09Hz and 2.35Hz. The frequency 1.09Hz corresponds to one cell and 2.35Hz is relevant to two cell. This two different frequencies are combined in pressure fluctuation signal. As flow rate decreases (from point a to d),

the pressure amplitude and frequency are increased. In case of the 40% contraction, rotating stall signal which less than rotational speed (5Hz) begin to be observed in operating point e. Both frequency peaks are 1.05 and 1.92 Hz. In the case of 53% contraction, pressure fluctuation disappears in operating point i. Pressure amplitude and periodicity of the fluctuation is noticeably reduced in compare to the case without contraction. In the case of 87% contraction, rotating stall not only disappears in operating point m, but also in operating point n. Pressure fluctuation decreases as flow rate decreases.

Figure 6 shows the secondary flow patterns observed in *r-z* plane at different operating point. In the case without contraction, two secondary vortices appear on both diffuser walls in operating point a as shown in Fig. 6(a). One is placed on the hub wall side around the exit of impeller and the other is located in the exit of diffuser. Flow discharged from the exit of impeller passes below the secondary vortex on hub side wall. Vortex size is almost half of distance between impeller and diffuser exit. Scroll vortex in collecting chamber appears in the exit of vaneless diffuser. In operating point b, two vortices exist in vaneless diffuser like in operating point a. However, the size of vortex becomes smaller than it of operating point a. Position of vortex core moves toward the exit of impeller. In operation point c where rotating stall is fully developed, four vortices appear along radial direction. The size of them is less than that of in operation point b. This secondary flow is because of low momentum of the hub side. Increasing of this low momentum region causes to the rotating stall.

Figure 6(b) presents the secondary flow patterns inside vaneless diffuser in the case with 40% contraction. In operation point e, discharging flow from the exit of impeller is blocked by the movable diffuser and passes through the gap between movable diffuser and hub wall. Flow passing along the hub wall is separated in trailing edge of the movable diffuser. This separated flow is reattached at r_o= 0.58 and clockwise vortex exists behind the movable diffuser. The flow above vortex is separated on the hub side wall of the diffuser exit again. The vortex in collecting chamber become stronger than that of the case without contraction. The vortex core moves to center of collecting chamber and has a developed shape in compare to the case without contraction. As flow rate decreases, vortex existing behind the movable diffuser is smaller and moves to the impeller exit. And then, in operation point g, three vortices is observed in vaneless diffuser.

This tendency is continued to the case of 50 % contraction as shown in Fig. 7(c). In operation point i, the vortex due to separation is formed behind the movable diffuser and another vortex is located in the exit of diffuser. As flow rate decreases, the size of vortices become smaller and their position moves to the impeller. In the case of 87% contraction, separation region after the movable diffuser extends and the size of it ranges r_o= 0.78. This is because the flow passing through gap between movable diffuse and the hub wall is greatly accelerated compare to the case of 43% and 50%.

CONCLUSION

This study is about the characteristics of rotating stall with contraction due to the movable diffuser. Results of that is summarized as follow.

1. In the case without contraction inside diffuser, rotating stall is caused by the separation region in hub side wall. The position of secondary vortex moves toward the exit of impeller and the size of it becomes smaller as rotating stall develops.
2. In the case with contraction inside diffuser, the separation region in rotating stall onset is disappeared but, the position of secondary flow vortex moves toward the exit of impeller and the size is reduced.
3. Contraction by inserting of the movable diffuser makes rotating stall delay. But, movable diffuser causes to total pressure drop at the exit of compressor.

REFERENCES

Jansen, W., 1964, " Rotating stall in Radial Vaneless diffuser," ASME Journal of basic engineering, December, pp. 750-758.

Fukushima, Y., Nishida, H., and Miura, H., 1989, “Rotating stall of Centrifugal Compressors,” Turbomachinery,17,No.3, pp149-159

Abdelhamid, A.N.,1982, “Control of Self-excited flow Oscillations in Vaneless Diffuser of Centrifugal Compressor system ,”ASME Paper No. 82-GT-188

Senoo, Y., Hayami, H., and Ueki, H., 1983 “Low-Solidity Tandem-Cacade Diffusers for Wide-Flow-Range Centrifugal Blowers,” ASME Paper No. 83-GT-3

Harada,H.,1996, “ Non-Surge Centrifugal Compressor with Variable Angle Diffuser Vanes,” Turbomachinery,24,No.10, pp.600-608

Kurokawa, J., Matsui, J., Kitahora, T., and Saha, L., 1997, “ A New Passive Device to Control Rotating Stall in Vaneless and Vaned Diffusers by Radial Grooves, ” Proc. JSME Intl. Conf. on Fluid engineering, pp. 1109-1114

Tsurusaki, H., and Kintahora, T., 1999, “Flow Control of Rotating Stall in a Radial Vaneless Diffuser, ” Proc. of 3rd ASME/JSME Joint Fluids engineering. Conf., Paper No. FEDSM99-1799

Masahiro, I., Daisaku, S., and Ueki,H., 2001 “Suppression of Rotating Stall by Wall Roughness Control in Vaneless Diffusers of Centrifugal Blowes,” J. Turbomachinery., Vol. 123, pp. 64-71

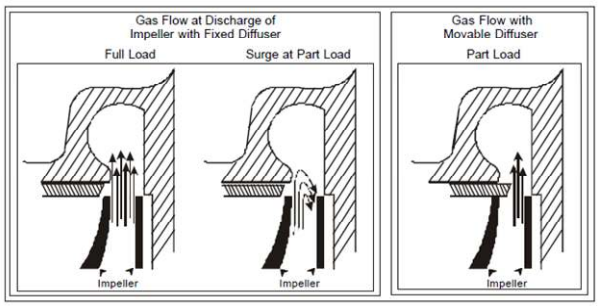

Figure. 1 Compressor movable diffuser used in McQuay Distinction^{TM} Chiller

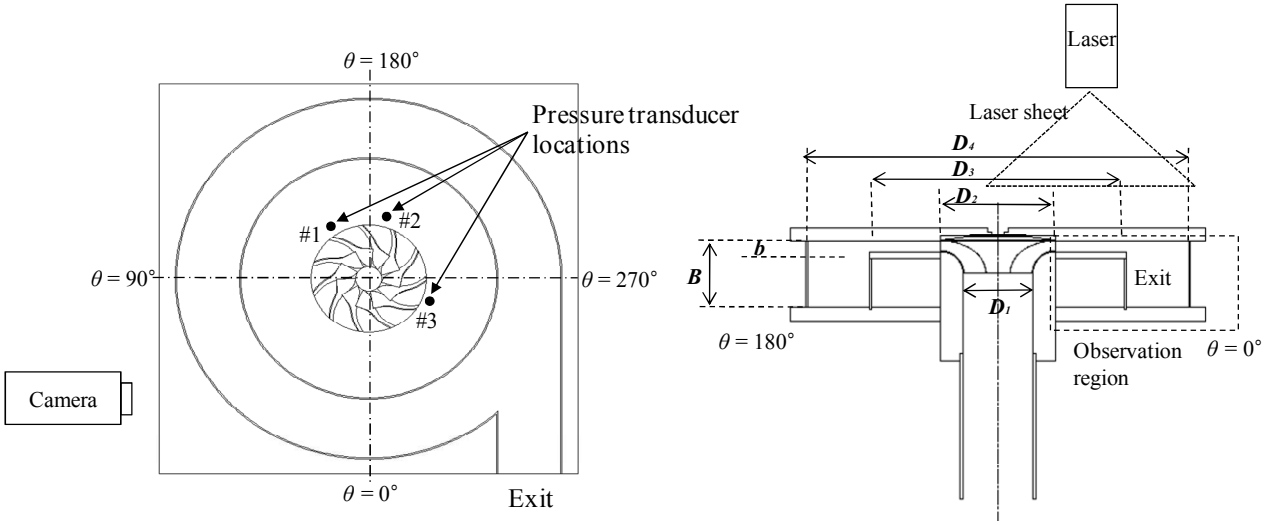

(a) Top view (*r*-θ plane) (b) Side view (*r*-*z* plane)

Figure. 2 Schematic of tested compressor

Table. 1 Specification of test rig

Designation (mm)	Size
D_1	97
D_2	165
D_3	370
D_4	550
B	90
b	16
t	2

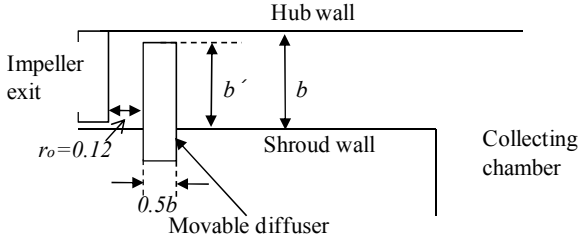

Figure. 3 Schematic of movable diffuser on shroud wall

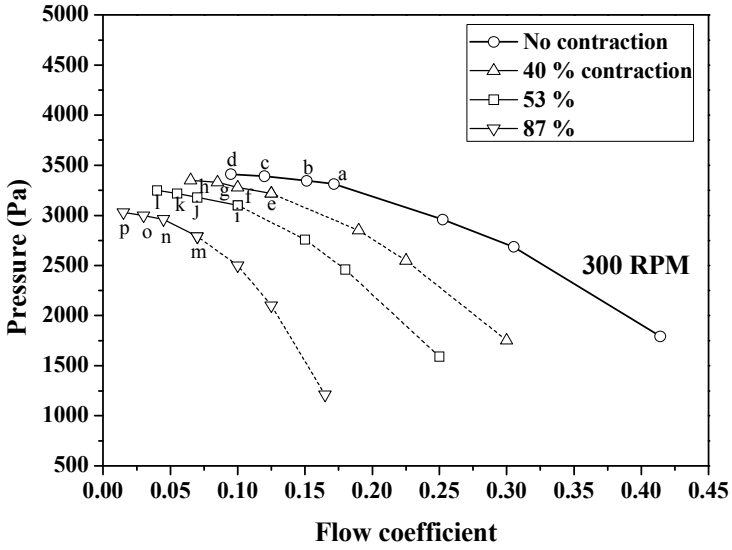

Figure. 4 Performance characteristics (Total pressure vs. mean velocity at compressor exit)

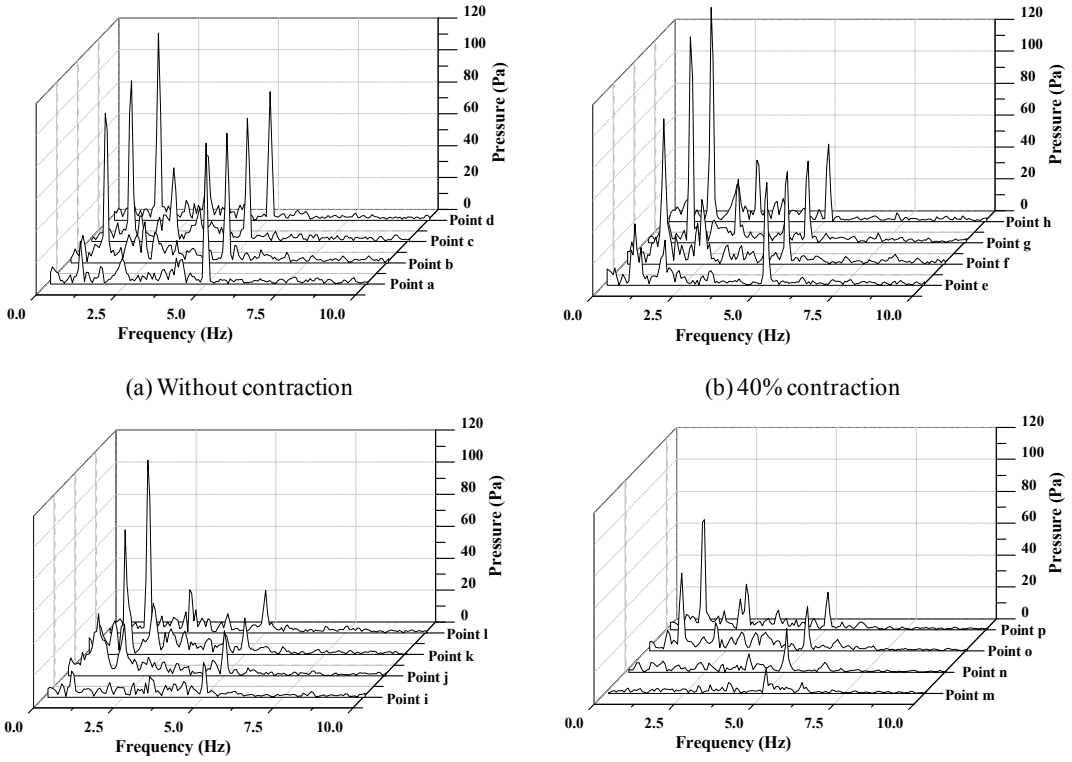

(a) Without contraction

(b) 40% contraction

(c) 53% contraction

(d) 87% contraction

Figure. 5 Frequency spectra of the pressure fluctuations at different operating point

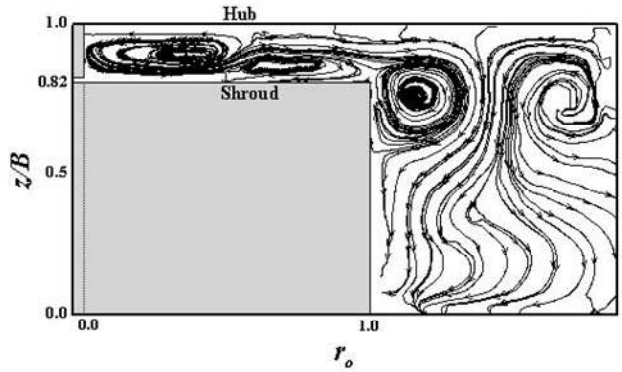

Operation point a

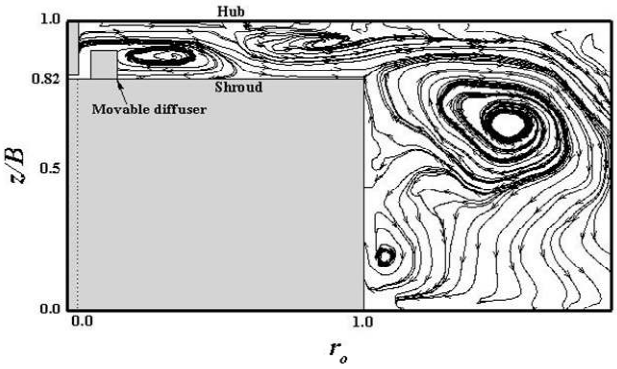

Operation point e

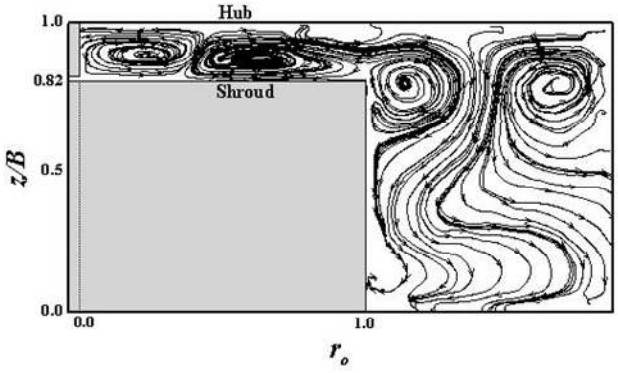

Operation point b

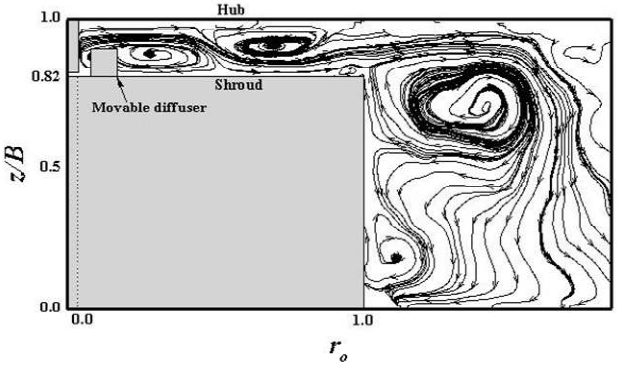

Operation point f

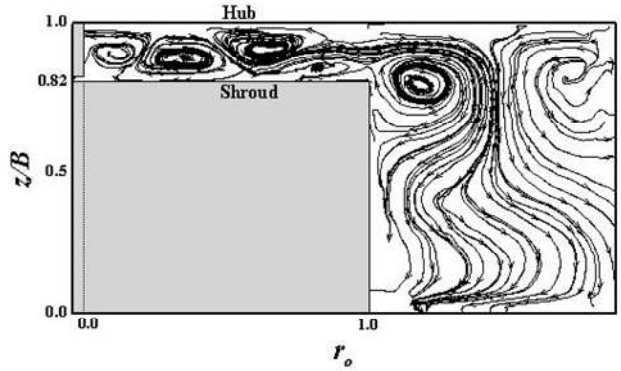

Operation point c

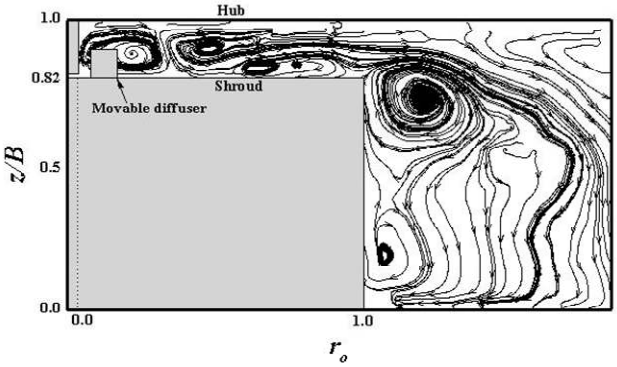

Operation point g

(a) No contraction (b) b´/b = 40 %

Figure. 6 Secondary flow pattern at different operating points

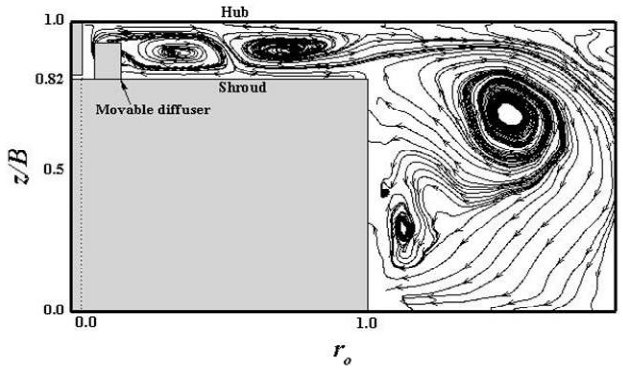

Operation point i

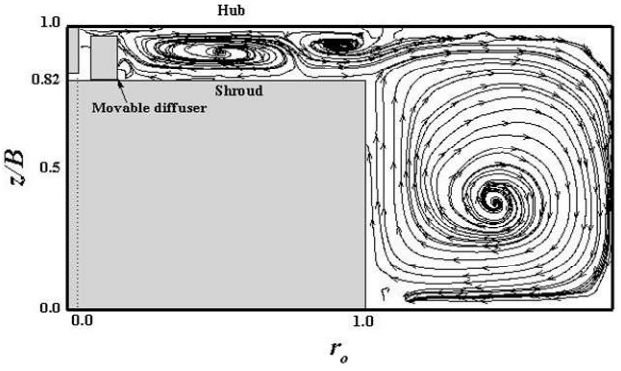

Operation point n

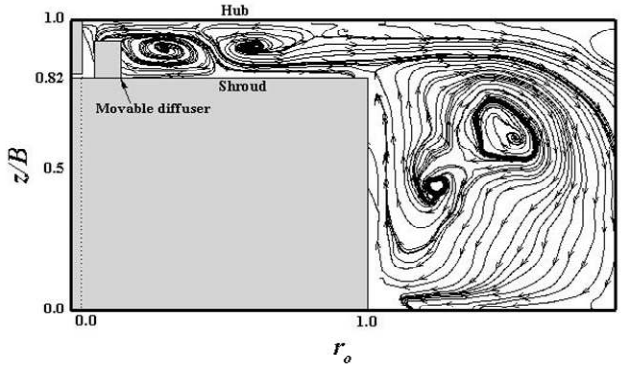

Operation point j

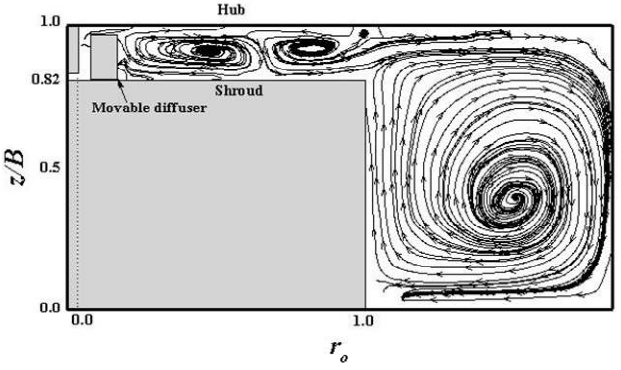

Operation point o

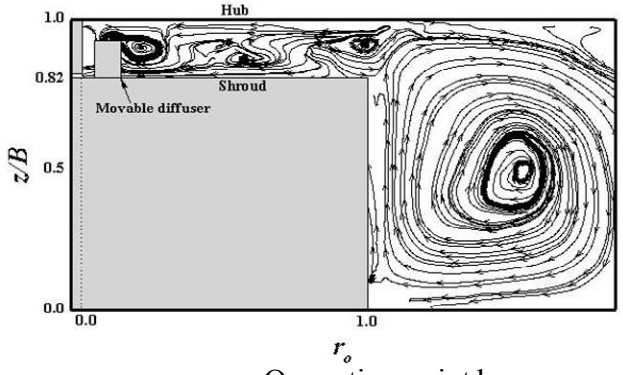

Operation point k

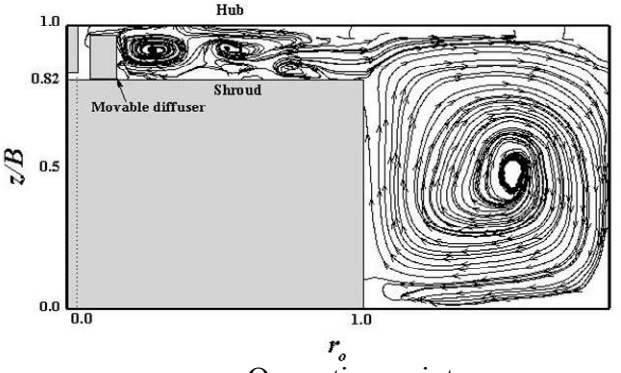

Operation point p

(c) b´/b = 53 %

(d) b´/b = 87 %

Figure. 7 Secondary flow pattern at different operation points